THE JOURNAL OF BIOLOGICAL CHEMISTRY VOL. 287, NO. 12, pp. 9213–9221, March 16, 2012

Functional Association of Catalytic and Ancillary Modules Dictates Enzymatic Activity in Glycoside Hydrolase Family 43 β-Xylosidase*

Received for publication, October 16, 2011, and in revised form, January 19, 2012 Published, JBC Papers in Press, January 23, 2012, DOI 10.1074/jbc.M111.314286

Sarah Moraïs[‡§1], Orly Salama-Alber[‡], Yoav Barak[‡¶], Yitzhak Hadar[§], David B. Wilson[‖], Raphael Lamed[**], Yuval Shoham[‡‡2], and Edward A. Bayer[‡3]

From the [‡]Department of Biological Chemistry, Weizmann Institute of Science, Rehovot 76100, Israel, the [§]Faculty of Agricultural, Food, and Environmental Quality Sciences, Hebrew University of Jerusalem, P. O. Box 12, Rehovot 76100, Israel, the [¶]Chemical Research Support, Weizmann Institute of Science, Rehovot 76100, Israel, the [‖]Department of Molecular Biology and Genetics, Cornell University, Ithaca, New York 14853, the [**]Department of Molecular Microbiology and Biotechnology, Tel Aviv University, Ramat Aviv 69978, Israel, and the [‡‡]Department of Biotechnology and Food Engineering, Technion-Israel Institute of Technology, Haifa 32000, Israel

Background: *Thermobifida fusca* β-xylosidase Xyl43A contains a catalytic and an ancillary module.
Results: Enzymatic activity is lost when the modules are expressed independently but is restored upon specific noncovalent re-association.
Conclusion: The catalytic and ancillary modules of Xyl43A behave as a single functional entity.
Significance: Two phylogenetically distinct modular components of an enzyme evolved together to form an enzymatically active unit.

β-Xylosidases are hemicellulases that hydrolyze short xylo-oligosaccharides into xylose units, thus complementing endoxylanase degradation of the hemicellulose component of lignocellulosic substrates. Here, we describe the cloning, characterization, and kinetic analysis of a glycoside hydrolase family 43 β-xylosidase (Xyl43A) from the aerobic cellulolytic bacterium, *Thermobifida fusca*. Temperature and pH optima of 55–60 °C and 5.5–6, respectively, were determined. The apparent K_m value was 0.55 mM, using *p*-nitrophenyl xylopyranoside as substrate, and the catalytic constant (k_{cat}) was 6.72 s^{-1}. *T. fusca* Xyl43A contains a catalytic module at the N terminus and an ancillary module (termed herein as Module-A) of undefined function at the C terminus. We expressed the two recombinant modules independently in *Escherichia coli* and examined their remaining catalytic activity and binding properties. The separation of the two Xyl43A modules caused the complete loss of enzymatic activity, whereas potent binding to xylan was fully maintained in the catalytic module and partially in the ancillary Module-A. Nondenaturing gel electrophoresis revealed a specific noncovalent coupling of the two modules, thereby restoring enzymatic activity to 66.7% (relative to the wild-type enzyme). Module-A contributes a phenylalanine residue that functions as an essential part of the active site, and the two juxtaposed modules function as a single functional entity.

Xylan is the major constituent of hemicellulose, which represents 20–30% of lignocellulosic plant biomass (1) and represents an important industrial target for degradation (*e.g.* bleaching in the pulp and paper industry (2)). Xylan is a linear polysaccharide, consisting of β-1,4 linked D-xylose units with a large variety of side-chain substituents. Consequently, the contribution of multiple hemicellulases is required for complete hydrolysis of xylan by synergistically complementary enzymes.

The well studied aerobic thermophilic soil bacterium, *Thermobifida fusca*, can use cellulose and xylan as sole carbon sources (3, 4). For this purpose, the bacterium produces a set of six cellulases and several hemicellulases such as xylanases, a β-xylosidase, an α-L-arabinofuranosidase, and an acetyl xylan esterase (5, 6). Two *T. fusca* endoxylanases (Xyn11A and Xyn10B) have been expressed and fully characterized (7, 8). A third endoxylanase, Xyn10A, was characterized from a related species *Thermomonospora alba* (9), and a nearly identical gene coding for this enzyme was found in *T. fusca*. Because of their potential industrial applications, the cloning and characterization of other thermostable xylanases deserve particular attention. We have therefore investigated in this communication the putative hemicellulase encoded by the *T. fusca* gene *tfu1616*, which was related in sequence to the family GH43 glycoside hydrolases (GH43), the members of which are known to possess β-xylosidase (EC 3.2.1.37), β-1,3-xylosidase (EC 3.2.1.72), α-L-arabinofuranosidase (EC 3.2.1.55), arabinanase (EC 3.2.1.99), xylanase (EC 3.2.1.8), or galactan 1,3-β-galactosidase (EC 3.2.1.145) activities (10). To date, over 1500 bacterial genes have been associated with this family. Over 50 bacterial enzymes from this family have been examined for their enzy-

* This work was supported in part by grants from the United States-Israel Binational Science Foundation, Jerusalem, Israel, Israeli Centers of Research Excellence (I-CORE) Program (Center 152/11), Alternative Energy Research Initiative Bioenergy Consortium, Brazilian friends of the Weizmann Institute of Science Alternative Energy Research Initiative (research grants from Charles Rothschild, Mario Fleck, and Roberto and Renata Ruhman), Technion-Niedersachsen Research Cooperation Program, and Israel Science Foundation Grants 966/09, 159/07, and 24/11.
[1] Recipient of scholarship from the Ministry of Immigrant Absorption, Jerusalem, Israel.
[2] Holds the Erwin and Rosl Pollak Chair in Biotechnology at Technion.
[3] Incumbent of The Maynard I. and Elaine Wishner Chair of Bio-organic Chemistry. To whom correspondence should be addressed. Tel.: 972-8-934-2373; Fax: 972-8-946-8256; E-mail: ed.bayer@weizmann.ac.il.

matic activities, but only a part of them have been fully characterized, the results of which were published in the primary literature. Among them, β-xylosidases (11–16), endoxylanases (17, 18), arabinanases (19–22), arabinofuranosidases (23–25), and galactanases (26) were described.

This study reports the cloning of the *tfu1616* gene of *T. fusca* and the characterization of the protein. The gene was expressed in *Escherichia coli*, and the protein was purified to near homogeneity. Data on physicochemical parameters and enzyme activity of the intact Xyl43A are provided. The two modules of the protein (a GH43 catalytic module and an associated ancillary module, Module-A) were produced as separate protein entities; the catalytic and binding activities were studied for both the separated modules as well as their *in vitro* combined form.

EXPERIMENTAL PROCEDURES

Cloning—Xyl43A (*tfu1616*, GenBank™ accession number AAZ555651) was cloned from *T. fusca* YX genomic DNA. Primers were designed with the program Oligo Primer Analysis Software version 5.1 and ordered at the Weizmann Institute of Sciences facility (N-terminal primer 5′-TCATGA**CATATG**CACCATCACCATCACCATACTTCTCCCCAAGTCACGTCCT-3′ and C-terminal primer 5′-TGATTG**CTCGAG**TTAGGAGGGGGACTGAGGCCGGTA-3′ (NdeI and XhoI sites in boldface). The PCR product was inserted and ligated into linearized pET21a to form pXyl43A.

GH43 was cloned using Xyl43A WT forward primer and 5′-TACGCT**CTCGAG**CTACGGCCACGGGTGCGGGG-3′ as a reverse primer (XhoI site in boldface) and Module-A using 5′-TTAAGC**CATATG**CAGCCGTCAGAGACCGACCACTTCGACGA-3′ and 5′-TTATGT**CTCGAG**GGAGGGGGACTGAGGCCGGT-3′ (NdeI and XhoI sites in boldface).

PCRs were performed using ABgene Reddymix x2 (Advanced Biotechnologies Ltd., Epsom, UK). DNA samples were purified using a HI Yield™ Gel/PCR fragments extraction kit (Real Biotech Corp., Banqiao City, Taiwan).

PCR mutagenesis was performed for the preparation of Xyl43A(F518A) and Module-A(F518A) plasmids using phosphorylated primers 5′-GGTGCCACGGGAGCGTTCCTCGGCCTGTGGG-3′ and 5′-CCACATGATGGGGTCGTTGC-3′ (ordered from Syntezza Bioscience Ltd., Jerusalem), and PCRs were performed using *Pfu* UltraII DNA polymerase (Agilent Technologies, Santa Clara, CA).

Protein Expression and Purification—Plasmids containing genes coding for the full-length Xyl43A enzyme, the GH43 module, ancillary Module-A, and mutants Xyl43A(F518A) and Module-A(F518A) were expressed in *E. coli* BL21 (lDE3) pLysS cells, and the expressed His-tagged proteins were purified on a nickel-nitrilotriacetic acid column (Qiagen), as reported earlier (27). A gel filtration purification step was conducted for association of the GH43 module and the Module-A, using an AKTAprime system and a Hiload 16/60 Superdex 75 column (GE Healthcare). SDS-PAGE was employed to test the purity of the recombinant proteins (12% acrylamide gels). The fractions with the highest degree of purity were pooled, and the concentrations of the recombinant proteins were estimated by absorbance at 280 nm based on their amino acid composition using the ProtParam program. Proteins were stored in 50% (v/v) glycerol at −20 °C.

Substrates—Microcrystalline cellulose (Avicel) was purchased from FMC Biopolymer (Philadelphia, PA) and was used for the preparation of phosphoric acid swollen cellulose (PASC 7.5 mg ml^{-1}, pH 7). Insoluble xylan was prepared by boiling oat-spelt xylan (Sigma) for 30 min in distilled water and recovering the pellet by centrifugation; this was followed by three cycles of washes with distilled water to remove soluble sugars and determination of dry weight (28). Birchwood xylan, beechwood xylan, chitin, *p*-nitrophenyl-β-D-glucopyranoside, *p*-nitrophenyl-α-L-arabinofuranoside, *p*-nitrophenyl-β-D-cellobioside, *p*-nitrophenyl-β-D-xylopyranoside (pNPX)[4] and xylobiose were purchased from Sigma. Debranched linear arabinan was purchased from Megazyme International, Ltd. (Wicklow, Ireland). Hatched wheat straw (0.2–0.8 mm) was provided by Valagro (Poitiers, France) and treated as described previously (29, 30).

pH Studies—The β-xylosidase activity over a pH range of 3.5–10 was investigated using citrate buffer from 3.5 to 8, Tris buffer from 7 to 9, and glycine/NaOH buffer from 9 to 10. Xyl43A was assayed at 50 °C for 7 min in a 700-μl reaction mixture containing 0.05 μM enzyme, 100 mM buffer, 1 mg/ml bovine serum albumin (BSA), and 5 mM pNPX. After 7 min, the tubes were placed on ice; the reaction was terminated by adding 200 μl of 1 M NaOH, and the absorbance was measured at 420 nm.

Temperature Dependence and Stability—The influence of temperature upon activity was assayed as follows. The release of *p*-nitrophenol by 0.05 μM Xyl43A at temperatures ranging from 30 to 80 °C was measured at 420 nm after a 7-min reaction and 15 min cooling on ice-water in a 700-μl final volume (100 mM buffer citrate, pH 6, 1 mg/ml BSA, 5 mM pNPX). The effect of temperature on the stability of Xyl43A was determined by incubating the enzyme without substrate over a 15-min period for 50 h at 50, 60, and 70 °C at pH 6. Similarly, the purified GH43 catalytic module, and Module-A were incubated at 50 °C over the same time period, either before or after combining the GH43/Module-A at 1:0.8 molar ratio. After adding substrates, 7-min reactions (as specified above) were carried out at 50 °C. The absorbance at 420 nm was then measured after a 15-min incubation on ice.

Kinetic Studies—Temperature-equilibrated reactions of a 180-μl final volume (100 mM buffer citrate, pH 6, 1 mg/ml BSA, 0–15 mM pNPX at 50 °C) were initiated by adding 10 μl of the enzyme (final concentration of 0.05 μM). The absorbance was monitored at 420 nm at 14-s intervals for 10 min, using an ELISA plate reader (BioTek Synergy HT, Winooski, VT). Absorbances (420 nm) were then converted to molarities using an extinction coefficient of 3365 $M^{-1} \cdot cm^{-1}$ for the absorbance of *p*-nitrophenol in citrate buffer, pH 6, at 50 °C.

Effect of Salts and Chemicals—Various salts and chemicals were added at a final concentration of 1 mM to the standard enzymatic reaction mixtures to check potential inhibitory effects on enzymatic activity.

[4] The abbreviations used are: pNPX, *p*-nitrophenyl-β-D-xylopyranoside; CBM, carbohydrate-binding module.

Binding to Insoluble Polysaccharides—The binding of the proteins to insoluble xylan and microcrystalline cellulose was determined qualitatively using SDS-PAGE. In a final volume of 100 μl, 10 μg (5 μg for cellulose binding experiments) of pure protein in 50 mM citrate buffer, pH 6.0, containing 12 mM $CaCl_2$ and 2 mM EDTA was mixed with 0.5 mg of insoluble xylan (or 10 mg of microcrystalline cellulose). Tubes were mixed gently at 4 °C for 1 h and centrifuged at 14,000 rpm for 1 min. The supernatant fluids (containing the unbound fraction of the proteins) were transferred to new tubes and supplemented with SDS-containing buffer. The pellets (containing the bound fraction of the proteins) were washed once by resuspension in 100 μl of the above-described buffer, centrifuged, and resuspended in 60 μl of SDS-containing buffer. Boiled samples were subjected to SDS-PAGE (12% gels) for analysis. BSA served as a negative control for binding specificity.

Thin Layer Chromatography (TLC)—The hydrolysis of xylobiose by Xyl43A was monitored by TLC analysis. The xylobiose hydrolysis reaction included 5 mg of xylobiose, 0.2 mM Xyl43A, and 100 mM citrate buffer, pH 6. The reaction was performed at 50 °C, and at different time points (5, 15, and 30 min and 2 h), samples were taken, and the reaction was terminated by adding Hg^{2+} to a final concentration of 1 mM (which completely inhibits the enzyme). Chromatography was carried out on Silica Gel 60 plates (Merck), using butanol/ethanol/water (3:2:2) as a developing solvent. Spots were visualized by charring with 0.2% orcinol (in methanol and 20% phosphoric acid in methanol, 1:1 v/v) and heating for 2 min at 150 °C.

Multiple Amino Acid Sequence Alignment—The Clustal W2 program was employed to analyze the amino acid sequence-based alignment between the characterized β-xylosidases in glycoside hydrolase family 43 (11–16) and *T. fusca* Xyl43A. This alignment served to identify the homologous conserved residues between *Geobacillus stearothermophilus* and *T. fusca* β-xylosidases that appear to be involved in the interface between the catalytic and the C-terminal Module-A of Xyl43A.

RESULTS

Sequence Analysis and Production of Xyl43A (tfu1616)—The gene encoding for Xyl43A is part of the hemicellulolytic system of *T. fusca*. It encodes a 550-amino acid protein with a calculated molecular mass of 61,686 Da. The amino acid sequence of the Xyl43A protein was subjected to BLAST analysis (blastp, nr data base, blast.ncbi.nlm.nih.gov) and showed significant homology (from 44 to 59% sequence identity) to β-xylosidases and α-L-arabinofuranosidases that belong to glycoside hydrolase family 43. The ORF has a G + C content of 68.4%, not significantly different from that (67%) of the whole genome of *T. fusca,* which is typical of many thermophilic organisms (31). The gene encoding for Xyl43A does not include any recognizable signal peptide as determined by the SignalP server. Thus, the protein is assumed to remain intracellularly in *T. fusca*. SDS-PAGE analysis of the purified Xyl43A protein revealed a single protein band of about 60 kDa, which is in good agreement with the calculated molecular mass. A typical Xyl43A preparation yielded 31.2 mg/liter purified protein.

Bioinformatic analysis of the protein revealed the presence of a GH43 catalytic module located between residues 16 and 319 and a second module of undefined function (ancillary module, Module-A) located between residues 338 and 550 in the C-terminal part of the protein. To evaluate the binding properties and the enzymatic activity of both N-terminal (catalytic core) and C-terminal (ancillary) modules, we produced two distinct chimeras, GH43 and Module-A. Because there is 45% identity and 60% similarity between the previously characterized GH43 from *G. stearothermophilus* (15, 32), its structure was used and compared with the predicted structure of *T. fusca* Xyl43A, obtained using Swiss Model (Fig. 1). The quality of the model was estimated using the ProSA-web site. The Z-score of the model was −6.57, which is well within the range of scores typically found for native proteins of similar size.

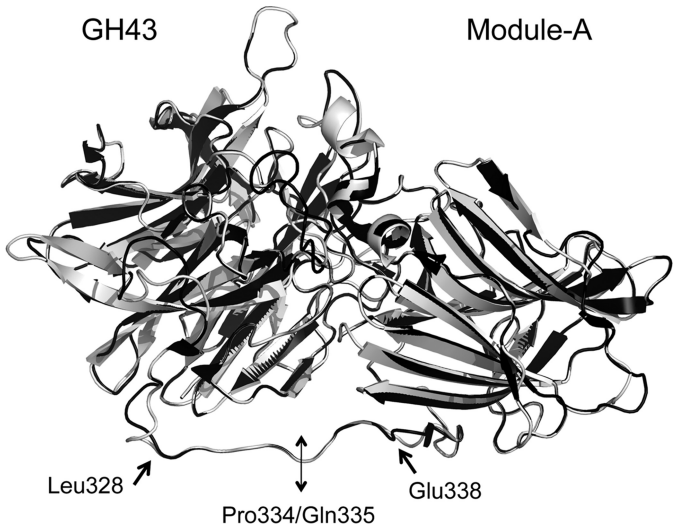

FIGURE 1. **Superposition of the solved structure of *G. stearothermophilus* XynB3 and the predicted model of *T. fusca* Xyl43A.** The known structure of *G. stearothermophilus* XynB3 (2exh) is shown in *black* and the predicted structure of *T. fusca* Xyl43A, determined using Swiss model, in *gray*. Amino acid residues delimiting the linker portion (Leu-328 and Glu-338) are given as well as the residues (Pro-334/Gln-335) where the N-terminal catalytic module and C-terminal module were separated.

The model was especially helpful for determining the linker region of *T. fusca* Xyl43A. In *G. stearothermophilus,* the linker extends from Val-319 to Asp-329; by analogy, we deduced that the linker region in *T. fusca* Xyl43A would extend similarly from Leu-328 to Glu-338. The most appropriate juncture between the two modules was determined to be the bond between the adjacent Pro-334 and Gln-335, where there seemed to be little or no interactions between the linker and the modules in the predicted model. The two modules were therefore cloned separately (each with an N-terminal His tag), expressed, and purified by metal ion affinity chromatography. The resultant GH43 module and ancillary Module-A exhibited their expected molecular masses (35.8 and 25.9 kDa, respectively) in the SDS-polyacrylamide gel, and purity above 95% was estimated (data not shown). A schematic representation of the recombinant proteins expressed in this study is shown in Fig. 2.

Substrate Specificity—The activity of the recombinant enzyme was tested on a variety of substrates. No enzymatic activity was detected on xylans (from birch wood, beech wood, and oat-spelt, both soluble and insoluble), cellulosic substrates (Avicel and PASC), chitin, wheat straw, arabinan *p*-nitrophenyl-β-D-glucopyranoside, *p*-nitrophenyl-β-D-cello-

bioside, and *p*-nitrophenyl-α-L-arabinofuranoside. Detectable levels of hydrolysis were only observed for pNPX and xylobiose, confirming that the enzyme belongs to the β-xylosidase class. Residual activity (k_{cat}/K_m of 0.75 s^{-1}·mM^{-1} *versus* 12.25 for pNPX) was observed with *p*-nitrophenyl-α-L-arabinofuranoside, due to the structural similarity between β-D-xylopyranoside and α-L-arabinofuranoside. These results support the premise that the conserved arginine (position 288 in *T. fusca* Xyl43A) allows the distinction between β-xylosidase and arabinofuranosidase classes (32). This arginine is believed to be conserved only in β-xylosidases. Neither the GH43 nor Module-A alone had measurable activities on any substrates (including xylans and arabinoxylan).

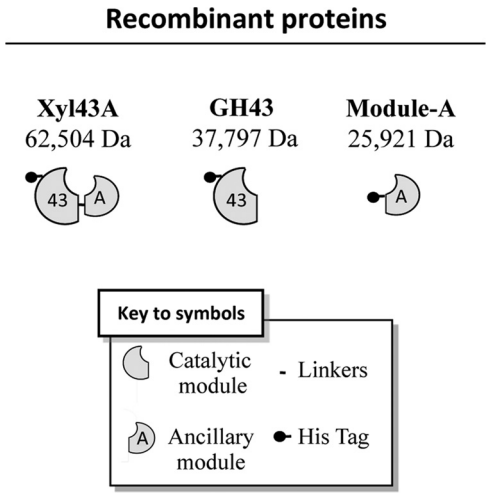

FIGURE 2. **Schematic representation of the recombinant proteins used in this study and their calculated molecular masses.**

pH Studies—The optimal pH range of Xyl43A was 5.5–6 for β-xylosidase activity (Fig. 3*A*) with more than 70% activity retained at pH 4.5 and 7. Xyl43A is more stable at alkaline pH than at acidic pH and is drastically inactivated at pH 4. It is indeed known that changes in pH affect the ionic or electric charge of active site amino acids (that participate in substrate binding and catalysis) and either enhance and stabilize interactions with the substrate or break intra- and intermolecular bonds, changing the shape of the enzyme, therefore affecting its efficacy (33). Activity profiles of glycosidases *versus* pH are typically bell-shaped, reflecting the ionization state of, at least, two essential amino acids residues. The expected pK_a values of the general base and general acid ionizable groups in the enzyme (derived from the pH-dependence graph) are 4.5 and 8, respectively, close to the values obtained for *G. stearothermophilus* XynB3 (15).

Thermostability—The hydrolysis rate increased from 30 to 60 °C, and the temperature coefficient (Q_{10}) was calculated to be 1.3. An Arrhenius plot exhibited a straight line from 30 to 60 °C, typical of a single rate-limited thermally activated process, indicating an increase in enzyme activity with increasing temperature. The activation energy and the pre-exponential factor were determined to be 18.9 kJ·mol^{-1} and 390, respectively. Under the reaction conditions, the temperature optimum was found to be 55–60 °C for β-xylosidase activity (Fig. 3*B*); however, the enzyme underwent rapid inactivation at 60 °C (Fig. 3*C*). Purified Xyl43A demonstrated moderate thermostability, and even after 50 h at 50 °C, 70% of the β-xylosidase activity remained. Incubation at 60 °C resulted in about 50% loss of activities after only 2 h and almost no activity after 24 h.

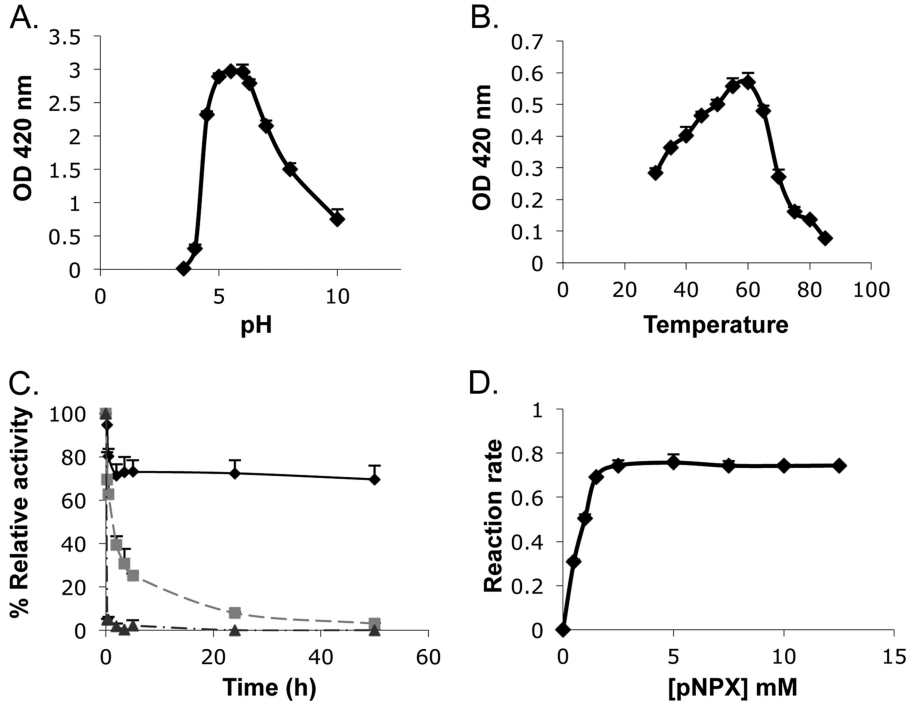

FIGURE 3. **Characterization of recombinant *T. fusca* Xyl43A.** *A,* effect of pH on β-xylosidase activity. *B,* effect of temperature on β-xylosidase activity. *C,* thermostability of Xyl43A β-xylosidase activity at different incubation temperatures, 50 (♦), 60 (■), and 70 °C (▲) at pH 6. *D,* effect of substrate concentration on β-xylosidase activity. Unless otherwise stated, the reactions were monitored for 10 min at 50 °C, pH 6. Reaction rates are given in μmol of *p*-nitrophenol·s^{-1} × 10^6. Reactions were performed in triplicate, and standard deviations are indicated.

TABLE 1
Effect of various chemicals at a concentration of 1 mM on Xyl43A activity
Relative activity is shown in % ± S.D.

Chemical	Relative activity	Chemical	Relative activity
	%		%
None	100	$CuSO_4$	81 ± 3
LiCl	98 ± 3	$AgNO_3$	10 ± 1
NaCl	91 ± 2	$ZnCl_2$	100
KCl	92 ± 5	$HgCl_2$	8 ± 4
$MgCl_2$	89 ± 5	EDTA	100
$CaSO_4$	86 ± 1	SDS	80 ± 1
$FeSO_4$	91 ± 4	Urea	78 ± 6
$MnCl_2$	85 ± 6	Citric acid	73 ± 2
$CoCl_2$	96 ± 1	Boric acid	61 ± 4

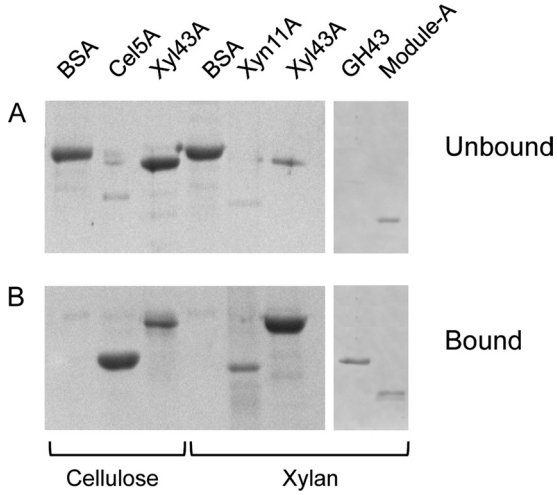

FIGURE 4. **Binding of the proteins to insoluble polysaccharides as assessed by SDS-PAGE.** *A,* unbound fractions; *B,* bound fractions. Each gel was loaded in the following order: BSA, Cel5A, Xyl43A, BSA, Xyn11A, Xyl43A, GH43, and Module-A. *1st to 3rd lanes,* binding experiment with microcrystalline cellulose; *4th to 8th lanes,* interactions with insoluble xylan.

Treatment at 70 °C resulted in complete inactivation of the enzyme in less than 15 min (Fig. 3*C*).

Kinetic Constants—The kinetic constants of Xyl43A on pNPX were determined by running the reaction at different substrate concentrations (Fig. 3*D*). At 50 °C and at pH 6, the release of *p*-nitrophenol was linear with time and proportional to enzyme concentration. The apparent K_m value was 0.55 mM pNPX, and the k_{cat} was 6.72 s^{-1}.

Effect of Various Chemicals—The effects of different chemicals on Xyl43A activity are shown in Table 1. The enzyme retained almost full activity in the presence of 1 mM Li^+, Na^{2+}, K^+, Mg^{2+}, Ca^{2+}, Fe^{3+}, Mn^{2+}, Co^{2+}, Cu^{2+}, and the reagent SDS. The addition of EDTA had no effect on the activity, suggesting that no metals are needed for the enzyme reactions. Group IIb metals such as Hg^{2+} and Ag^{2+} gave stronger inhibition (mercury inhibition is indeed well known for most enzymes, including cellulases and xylanases, indicating the existence of essential thiol groups (7)).

Binding to Insoluble Polysaccharides—The binding capacity of Xyl43A to insoluble xylan and microcrystalline cellulose was investigated. Full-length Xyl43A exhibited strong binding capacity for insoluble xylan, whereas weak binding to microcrystalline cellulose was observed (Fig. 4). As expected, the bulk of the BSA negative control was found in the unbound fraction, and the respective insoluble xylan and microcrystalline cellulose-positive controls were located in the bound fractions. The GH43 catalytic module alone demonstrated full binding capacity for insoluble xylan, whereas Module-A was found in bound and unbound fractions in almost equal proportions. Thus, it seems that the xylan binding capacity of Xyl43A is due mainly to the residues present in the catalytic module, and the ancillary Module-A plays a minor role in the binding interaction (Fig. 4).

Re-association of GH43 and Module-A—Noncovalent association of the separately expressed and purified GH43 and Module-A components at room temperature was analyzed by nondenaturing PAGE. The catalytic module was mixed with increasing amounts of the helper module in molar ratios ranging from 1:0.2 to 1:1.8, and the mobility pattern of each mixture was compared with that of each module alone and with that of the full-length Xyl43A enzyme. Mixtures of GH43 and Module-A resulted in complex formation (Fig. 5*A*). The mobility pattern of the complex was nearly identical to that of wild-type Xyl43A, revealing a specific interaction between the catalytic and ancillary modules. The intensity of the band, corresponding to the interaction of GH43 and Module-A, increased until a 1:0.8 ratio (GH43/Module-A), whereas the intensity of the bands of each of the individual modules decreased. At this ratio, the Module-A band interacted completely with GH43. A relatively small part of the latter fails to form the complex, probably because of incorrect folding of a portion of the GH43 fraction. Up to 25% of the wild-type β-xylosidase activity was thus recovered upon association of the two modules (Fig. 5*B*).

Gel filtration was used to purify the reassociated enzyme from the two modules at a 1:0.8 ratio, and the kinetics parameters were determined for the purest fraction obtained. The apparent K_m value was 0.6 mM pNPX (similar to that of the wild-type enzyme), whereas the k_{cat} was 4.83 s^{-1}. Up to 71.8% of the wild-type β-xylosidase activity was thus recovered upon association of the two modules.

The moderate thermostability characteristics observed for the wild-type enzyme (Fig. 3*C*) raised the question as to whether the re-associated Xyl43A would also be stable to heat treatment under the same conditions. Moreover, it was of interest to determine whether exposure of the two constitutive modules to heat would result in reduced stability. We therefore subjected the two isolated modules to heat treatment at 50 °C both prior to and after re-association. Heat treatment of the two modules separately before re-association led to a marked loss of stability (Fig. 5*C*). About 60% of the residual activity was obtained after 2 h of heat treatment, and only 15% remained after 5 h. In contrast, re-association of the two modules before heat treatment resulted in increased thermostability; about 80% relative activity remained after 5 h of heat treatment and 50% after 48 h (Fig. 5*C*). The results indicated that the individual modules exhibit decreased stability in solution but upon re-association form a stable complex.

To gain insight into the molecular basis of re-association of the GH43 and Module-A, we employed the Protein Interaction Calculator server (34) to analyze the known three-dimensional structure of the family GH43 XynB3 β-xylosidase from *G. stearothermophilus*. Using this server, the various interactions involved in the interface between the catalytic and the C-terminal Module-A were determined, and the homologous con-

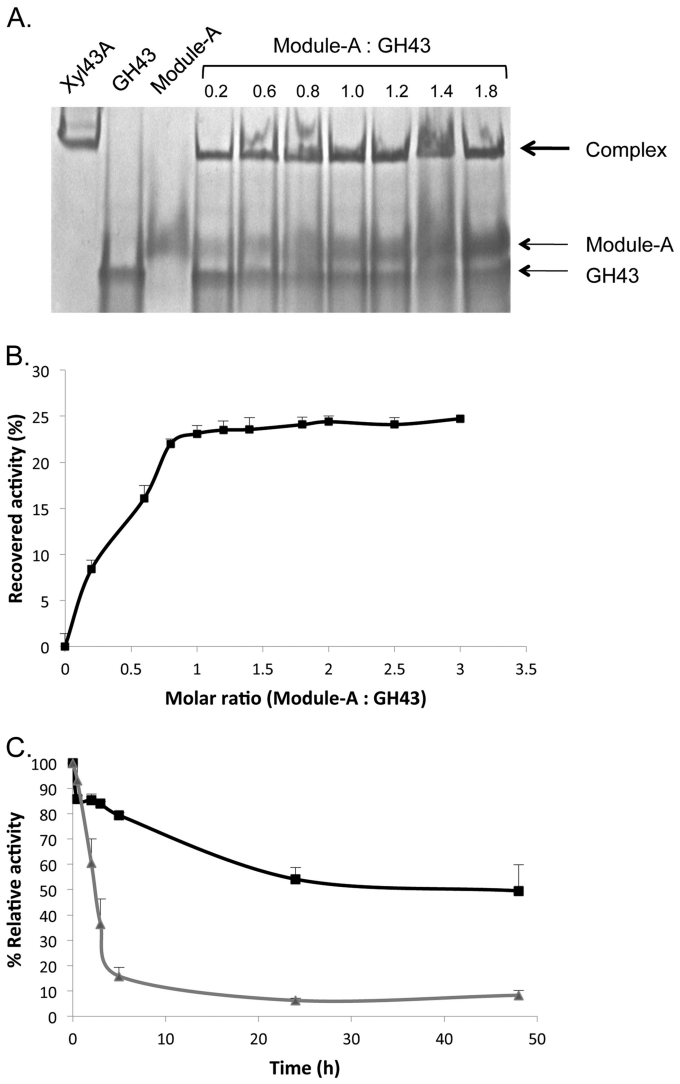

FIGURE 5. **Physical association of GH43 and Module-A.** *A,* specific association of GH43 and Module-A revealed by nondenaturing gel electrophoresis (7.5%). Mixtures of GH43 and Module-A (at the indicated molar ratio relative to GH43) were subjected to nondenaturing PAGE, and the mobility pattern of each mixture was compared with that of the individual modules and to wild-type Xyl43A. Mixtures of the two modules resulted in formation of a complex (*thick arrow*). *1st lane,* full-length Xyl43A enzyme (150 pmol); *2nd lane,* GH43 (150 pmol); *3rd lane,* Module-A (150 pmol); *4th to 10th lanes*, GH43 (150 pmol) mixed with increasing amounts of Module-A (30–290 pmol), at the indicated molar ratios. *B,* recovery of β-xylosidase activity upon association of GH43 and Module-A. A fixed amount (150 pmol) of the GH43 was mixed with increasing amounts of Module-A, and their respective activities were compared with that of the intact Xyl43A (set as 100%). *C,* thermostability of GH43, Module-A, and the re-associated form of Xyl43A over time at 50 °C and pH 6. Curves are labeled as follows: heat treatment of GH43 and Module-A prior to their interaction (*gray triangles*) and following re-association at a 1:0.8 molar ratio of GH43:Module-A (*black square*). Reactions were performed in duplicate, and standard deviations are indicated.

served residues in *T. fusca* Xyl43A were then identified. Table 2 shows the major residues, predicted to be involved in the intramodular interface. The data suggest strong reciprocal binding interaction between the two modules of *T. fusca* Xyl43A and provide an explanation for their observed re-association.

Production of Mutated Xyl43A(F518A)—According to the crystal structure of the family GH43 β-xylosidase (XynB3) from *G. stearothermophilus* T-6 (32), the active site of the enzyme possesses a pocket topology, mainly constructed from β-propeller domain residues. In addition, a conserved phenylalanine residue (Phe-518 of *T. fusca* Xyl43A, homologous to Phe-506 of *G. stearothermophilus* XynB3) is located on a loop of Module-A in the latter structure. The loop serves to close one side of a cleft, formed by the catalytic module, and inserts Phe-506 therein. This phenylalanine is the only residue in Module-A, which participates in the active site and presumably plays a role in substrate binding and specificity. To further investigate the role of this amino acid in the catalytic activity of *T. fusca* Xyl43A, the conserved Phe-518 was replaced with Ala.

TABLE 2
Major conserved residues likely to be involved in the strong binding interaction between the two modules of the *T. fusca* Xyl43A, based on the solved structure of *G. stearothermophilus*

	Intermodular interactions				
Residues	Hydrophobic	Hydrogen bonding	Ionic	Aromatic	Cation P_i
Phe-28	Phe-522	Arg-392		Phe-522	Arg-392
Trp-50				Tyr-420	
Tyr-51	Pro-357	Thr-353			
Lys-262			Asp-502		
Arg-296		Phe-518	Asp-502		Phe-518
Ser-352		Trp-50 (2)[a]			
		Pro-52 (2)			
Thr-353		Tyr-51			
Arg-355		Arg-83 (3)			
Thr-423		Asp-85 (2)			
Glu-503		Trp-225	Lys-262		
		Lys-262			
		Cys-292			
Phe-518	Phe-48			Phe-48	
	Trp-90			Trp-90	

[a] Number of interactions (greater than 1) of a given residue is shown parenthetically.

The kinetic constants of Xyl43A(F518A) for pNPX hydrolysis were determined by interaction of the mutant enzyme at different substrate concentrations as performed for the wild-type enzyme (data not shown). At 50 °C and pH 6, the release of *p*-nitrophenol was linear with time and proportional to enzyme concentration. The apparent K_m value was 0.98 mM pNPX, and the k_{cat} was 0.059 s^{-1}. The replacement of the phenylalanine by alanine affected the activity of the enzyme dramatically, the activity of the mutant representing less than 1% of the wild-type activity on pNPX (0.89%).

Re-association of GH43 and Mutated Module-A(F518A)—To further examine the role of the Phe-518 residue in the catalysis, Module-A was replaced with alanine in a manner similar to that of the wild-type enzyme. As described for the wild-type modules, noncovalent association of GH43 and the mutated Module-A(F518A) was performed. A strong interaction between the two modules was observed (data not shown), suggesting that Phe-518 does not play a dominant role in the strong association between the two modules. Nevertheless, upon association of the modules, β-xylosidase activity was not recovered, suggesting that the role of this particular amino acid is directly related to catalysis *per se*.

DISCUSSION

A number of GH43 family members (as well as GH3, GH51, and GH54 families) have been reported to exhibit simultaneously both β-xylosidase and α-L-arabinofuranosidase activities, probably because of the active site geometry that does not allow the enzyme to distinguish between the two saccharides. Indeed,

both activities seem to occur in the same active site (35, 36). The *T. fusca* Xyl43A, characterized here, exhibited primarily β-xylosidase activity and only nominal levels of α-L-arabinofuranosidase activity.

In previous research (37), Asp and Glu residues of family GH43 enzymes have been directly implicated in substrate hydrolysis, in line with the classical general acid (proton donor) and nucleophile/base that characterize enzymatic hydrolysis of the glycosidic bond (38). Multiple sequence alignment of glycoside hydrolase families 32, 43, 62, and 68 revealed three conserved blocks, each containing an acidic residue at an equivalent position in all of the enzymes; site-directed mutagenesis studies have shown that Asp/Glu (block I), Asp (block II), and Glu (block III) are essential for catalytic activity of GH43. This indicates direct involvement of the conserved residues in substrate binding and hydrolysis, and substitutions of these specific residues inactivate the enzyme or considerably reduce its activity. These three strictly conserved key acidic residues are located in a funnel-shaped active site that includes two subsites with a single route for access by ligands in a β-propeller architecture, and the three residues operate with the canonical reaction mechanism of inversion of anomeric configuration (32, 39). More recently, the crystal structures of *Cellvibrio japonicus* arabinanase 43A and *G. stearothermophilus* β-xylosidase further demonstrated the role of these three carboxylates in catalytic activity (19, 31). Similar blocks and essential residues were found in *T. fusca* Xyl43A by sequence comparison as follows: block I ^{29}YP**D**PS^{33}, block II ^{142}GF**D**PS^{146}, and block III ^{201}VT**E**APH^{206}.

In the GH43 family, several modular architectures are observed (40). One group of GH43 enzymes is composed only of a single GH43 module and lacks the C-terminal module (Module-A). These enzymes belong to the arabinanase class (20–22, 41). Another group of family GH43 enzymes comprising both modules is defined as either β-xylosidases or α-L-arabinofuranosidases (32, 42). One possibility is that the C-terminal module in family GH43 would be responsible for switching substrate specificity from arabinan to xylobiose. However, in this study, the *T. fusca* GH43 module alone was unable to degrade arabinan, and no binding ability of either of the two Xyl43A modules toward arabinan was observed, thus suggesting that the difference in specificities is a function of the topography and composition of the active site. According to Alhassid *et al.* (22), the topology of the active site in *G. stearothermophilus* T-6 arabinanase (AbnB) resembles a groove with a narrow bridge formed by Phe-104 (conserved in family GH43 arabinanases) and Cys-222. A neighboring cysteine (Cys-221) bridges with the Cys-222 and covers the cleft formed in the active site. The Phe and both Cys residues are absent from β-xylosidases in general, and *T. fusca* β-xylosidase in particular. Moreover, according to Brux *et al.* (32), in the β-xylosidases, an extended arabinopyranose ligand would clash with the hydrophobic area generated by conserved xylosidase residues, *i.e.* Trp-74, Phe-127, Phe-32, and Phe-506 of *G. stearothermophilus* XynB3. In the case of galactopyranose, there is also a steric clash caused by the additional hydroxymethyl group, which encounters Phe-506 (1.4 Å). These criteria explain the specificity of the *T. fusca* catalytic GH43 module and underscore the sophisticated divergence of the conserved GH43 arabinanases and β-xylosidases.

Physical separation and reassociation of the two modular components of Xyl43A (GH43 and Module-A) enabled us to further analyze the enzymatic and binding properties of this enzyme. Separating the two modules led to a complete loss in enzymatic activity of the N-terminal module GH43 but did not affect its ability to bind xylan, suggesting that the active site would thus need the combined conformation of the complete protein to degrade its substrate correctly. Indeed, a strong noncovalent interaction occurs between the two modules of *T. fusca* Xyl43A. This physical interaction led to substantial recovery of β-xylosidase activity (71.8%), demonstrating the role of the Module-A in enzymatic degradation of its substrate. Based on the solved structure of *G. stearothermophilus* (32, 43), several residues play an essential role in formation of the strong interface between the two modules of the enzyme (Table 2).

The re-association of GH43 and Module-A in *T. fusca* Xyl43A provided a key functional residue for β-xylosidase activity. The phenylalanine located at position 518 of Module-A was thus demonstrated to be inserted in a critical position and essential for Xyl43A enzymatic activity. The F518A replacement, either in the intact enzyme Xyl43A or in Module-A, resulted in the near-complete loss of enzymatic activity. According to Brux *et al.* (32), this conserved phenylalanine emerges from a loop originated from the β-sandwich domain and contributes to substrate binding by a stacking interaction with the xylose unit at the −1 subsite. Interestingly, the amino acid replacement does not appear to affect the overall folding of the enzyme according to the re-association of the separated GH43 and mutated Module-A.

In a recent article (44), physical re-association of a family GH9 endoglucanase catalytic module and its ancillary family 3c CBM was also demonstrated with attendant regain of enzyme activity. The latter study, together with this study, promotes the original description of the combined S-protein and S-peptide to generate an active form of ribonuclease A (45). In the current studies on the glycoside hydrolases, however, the two interacting modules are clearly of distinct evolutionary origin.

Indeed, the two separate modules of Xyl43A fold on their own, suggesting that originally they may have had distinct functions. The evolutionary source of the C-terminal Module-A, however, is unclear, because it is phylogenetically unconnected with any known protein in the databases other than those associated with the family GH43 enzymes. Perhaps an ancestral form of Module-A was originally a CBM, because it possesses reminiscent characteristics of a CBM (*e.g.* β-sandwich structure); its binding role would presumably have been lost during evolvement of its singular catalytic contribution to the GH43 xylosidases. Moreover, because Xyl43A does not contain any signal peptide, the enzyme appears to remain in the intracellular milieu in *T. fusca* and would not require a CBM to target the enzyme to its substrate. Indeed, xylobiose is small enough to enter the cell, presumably via an appropriate transport apparatus, and can be degraded internally into xylose units, so a CBM would be irrelevant for the enzyme. Consequently, as representative of the GH43 β-xylosidases, the two linked modules of *T. fusca* Xyl43A should thus be considered as an intact, syn-

chronized functional unit, rather than a fortuitous pair of independent modules.

Acknowledgments—We are grateful for the critique and assistance of Drs. Ilit Noach and Bareket Dassa (Weizmann Institute of Sciences, Rehovot, Israel) throughout the stages of preparation of the manuscript.

REFERENCES

1. Kulkarni, N., Shendye, A., and Rao, M. (1999) Molecular and biotechnological aspects of xylanases. *FEMS Microbiol. Rev.* **23,** 411–456
2. Beg, Q. K., Kapoor, M., Mahajan, L., and Hoondal, G. S. (2001) Microbial xylanases and their industrial applications. A review. *Appl. Microbiol. Biotechnol.* **56,** 326–338
3. Wilson, D. B. (1992) Biochemistry and genetics of actinomycete cellulases. *Crit. Rev. Biotechnol.* **12,** 45–63
4. Wilson, D. B. (2004) Studies of *Thermobifida fusca* plant cell wall-degrading enzymes. *Chem. Rec.* **4,** 72–82
5. Bachmann, S. L., and McCarthy, A. J. (1991) Purification and cooperative activity of enzymes constituting the xylan-degrading system of *Thermomonospora fusca*. *Appl. Environ. Microbiol.* **57,** 2121–2130
6. Ghangas, G. S., Hu, Y. J., and Wilson, D. B. (1989) Cloning of a *Thermomonospora fusca* xylanase gene and its expression in *Escherichia coli* and *Streptomyces lividans*. *J. Bacteriol.* **171,** 2963–2969
7. Irwin, D., Jung, E. D., and Wilson, D. B. (1994) Characterization and sequence of a *Thermomonospora fusca* xylanase. *Appl. Environ. Microbiol.* **60,** 763–770
8. Kim, J. H., Irwin, D., and Wilson, D. B. (2004) Purification and characterization of *Thermobifida fusca* xylanase 10B. *Can. J. Microbiol.* **50,** 835–843
9. Blanco, J., Coque, J. J., Velasco, J., and Martín, J. F. (1997) Cloning, expression in *Streptomyces lividans*, and biochemical characterization of a thermostable endo-β-1,4-xylanase of *Thermomonospora alba* ULJB1 with cellulose-binding ability. *Appl. Microbiol. Biotechnol.* **48,** 208–217
10. Cantarel, B. L., Coutinho, P. M., Rancurel, C., Bernard, T., Lombard, V., and Henrissat, B. (2009) The Carbohydrate-Active EnZymes database (CAZy). An expert resource for glycogenomics. *Nucleic Acids Res.* **37,** D233–238
11. Moriyama, H., Fukusaki, E., Cabrera Crespo, J., Shinmyo, A., and Okada, H. (1987) Structure and expression of genes coding for xylan-degrading enzymes of *Bacillus pumilus*. *Eur. J. Biochem.* **166,** 539–545
12. La Grange, D. C., Pretorius, I. S., and van Zyl, W. H. (1997) Cloning of the *Bacillus pumilus* β-xylosidase gene (*xynB*) and its expression in *Saccharomyces cerevisiae*. *Appl. Microbiol. Biotechnol.* **47,** 262–266
13. Chun, Y. C., Jung, K. H., Lee, J. C., Park, S. H., Chung, H. K., and Yoon, K. H. (1998) Molecular cloning and the nucleotide sequence of the *Bacillus* sp. KK1 beta-xylosidase gene. *J. Mol. Microbiol. Biotechnol.* **8,** 28–33
14. Whitehead, T. R., and Cotta, M. A. (2001) Identification of a broad-specificity xylosidase/arabinosidase important for xylooligosaccharide fermentation by the ruminal anaerobe *Selenomonas ruminantium* GA192. *Curr. Microbiol.* **43,** 293–298
15. Shallom, D., Leon, M., Bravman, T., Ben-David, A., Zaide, G., Belakhov, V., Shoham, G., Schomburg, D., Baasov, T., and Shoham, Y. (2005) Biochemical characterization and identification of the catalytic residues of a family 43 β-D-xylosidase from *Geobacillus stearothermophilus* T-6. *Biochemistry* **44,** 387–397
16. Smaali, I., Rémond, C., and O'Donohue, M. J. (2006) Expression in *Escherichia coli* and characterization of β-xylosidases GH39 and GH-43 from *Bacillus halodurans* C-125. *Appl. Microbiol. Biotechnol.* **73,** 582–590
17. Gosalbes, M. J., Pérez-González, J. A., González, R., and Navarro, A. (1991) Two β-glycanase genes are clustered in *Bacillus polymyxa*. Molecular cloning, expression, and sequence analysis of genes encoding a xylanase and an endo-β-(1,3)-(1,4)-glucanase. *J. Bacteriol.* **173,** 7705–7710
18. Bourgois, T. M., Van Craeyveld, V., Van Campenhout, S., Courtin, C. M., Delcour, J. A., Robben, J., and Volckaert, G. (2007) Recombinant expression and characterization of XynD from *Bacillus subtilis* subsp. *subtilis* ATCC 6051. A GH 43 arabinoxylan arabinofuranohydrolase. *Appl. Microbiol. Biotechnol.* **75,** 1309–1317
19. McKie, V. A., Black, G. W., Millward-Sadler, S. J., Hazlewood, G. P., Laurie, J. I., and Gilbert, H. J. (1997) Arabinanase A from *Pseudomonas fluorescens* subsp. *cellulosa* exhibits both an endo- and an exo-mode of action. *Biochem. J.* **323,** 547–555
20. Nurizzo, D., Turkenburg, J. P., Charnock, S. J., Roberts, S. M., Dodson, E. J., McKie, V. A., Taylor, E. J., Gilbert, H. J., and Davies, G. J. (2002) *Cellvibrio japonicus* α-L-arabinanase 43A has a novel five-blade β-propeller fold. *Nat. Struct. Biol.* **9,** 665–668
21. Leal, T. F., and de Sá-Nogueira, I. (2004) Purification, characterization, and functional analysis of an endo-arabinanase (AbnA) from *Bacillus subtilis*. *FEMS Microbiol. Lett.* **241,** 41–48
22. Alhassid, A., Ben-David, A., Tabachnikov, O., Libster, D., Naveh, E., Zolotnitsky, G., Shoham, Y., and Shoham, G. (2009) Crystal structure of an inverting GH 43 1,5-α-L-arabinanase from *Geobacillus stearothermophilus* complexed with its substrate. *Biochem. J.* **422,** 73–82
23. Matsuo, N., Kaneko, S., Kuno, A., Kobayashi, H., and Kusakabe, I. (2000) Purification, characterization, and gene cloning of two α-L-arabinofuranosidases from *Streptomyces chartreusis* GS901. *Biochem. J.* **346,** 9–15
24. van den Broek, L. A., Lloyd, R. M., Beldman, G., Verdoes, J. C., McCleary, B. V., and Voragen, A. G. (2005) Cloning and characterization of arabinoxylan arabinofuranohydrolase-D3 (AXHd3) from *Bifidobacterium adolescentis* DSM20083. *Appl. Microbiol. Biotechnol.* **67,** 641–647
25. Vandermarliere, E., Bourgois, T. M., Van Campenhout, S., Strelkov, S. V., Volckaert, G., Delcour, J. A., Courtin, C. M., and Rabijns, A. (2007) Crystallization and preliminary x-ray analysis of an arabinoxylan arabinofuranohydrolase from *Bacillus subtilis*. *Acta Crystallogr Sect. F Struct. Biol. Cryst. Commun.* **63,** 692–694
26. Ichinose, H., Yoshida, M., Kotake, T., Kuno, A., Igarashi, K., Tsumuraya, Y., Samejima, M., Hirabayashi, J., Kobayashi, H., and Kaneko, S. (2005) An exo-β-1,3-galactanase having a novel β-1,3-galactan-binding module from *Phanerochaete chrysosporium*. *J. Biol. Chem.* **280,** 25820–25829
27. Caspi, J., Irwin, D., Lamed, R., Shoham, Y., Fierobe, H. P., Wilson, D. B., and Bayer, E. A. (2006) *Thermobifida fusca* family-6 cellulases as potential designer cellulosomes components. *Biocat. Biotransform.* **24,** 3–12
28. Kluepfel, D., Vats-Mehta, S., Aumont, F., Shareck, F., and Morosoli, R. (1990) Purification and characterization of a new xylanase (xylanase B) produced by *Streptomyces lividans* 66. *Biochem. J.* **267,** 45–50
29. Fierobe, H. P., Mingardon, F., Mechaly, A., Bélaïch, A., Rincon, M. T., Pagès, S., Lamed, R., Tardif, C., Bélaïch, J. P., and Bayer, E. A. (2005) Action of designer cellulosomes on homogeneous *versus* complex substrates. Controlled incorporation of three distinct enzymes into a defined trifunctional scaffoldin. *J. Biol. Chem.* **280,** 16325–16334
30. Tabka, M. G., Herpoël-Gimbert, I., Monod, F., Asther, M., and Sigoillot, J. C. (2006) Enzymatic saccharification of wheat straw for bioethanol production by a combined cellulase xylanase and feruloyl esterase treatment. *Enzyme Microb. Technol.* **39,** 897–902
31. Kukolya, J., Nagy, I., Láday, M., Tóth, E., Oravecz, O., Márialigeti, K., and Hornok, L. (2002) *Thermobifida cellulolytica* sp. *nov.*, a novel lignocellulose-decomposing actinomycete. *Int. J. Syst. Evol. Microbiol.* **52,** 1193–1199
32. Brüx, C., Ben-David, A., Shallom-Shezifi, D., Leon, M., Niefind, K., Shoham, G., Shoham, Y., and Schomburg, D. (2006) The structure of an inverting GH43 β-xylosidase from *Geobacillus stearothermophilus* with its substrate reveals the role of the three catalytic residues. *J. Mol. Biol.* **359,** 97–109
33. Price, N. C., and Stevens, L. (2001) *Fundamentals of Enzymology: The Cell and Molecular Biology of Catalytic Proteins,* 3rd Ed., pp. 133–135, Oxford University Press, New York
34. Tina, K., Bhadra, R., and Srinivasan, N. (2007) PIC: Protein interactions calculator. *Nucleic Acids Res.* **35,** 473–476
35. Sakka, K., Yoshikawa, K., Kojima, Y., Karita, S., Ohmiya, K., and Shimada, K. (1993) Nucleotide sequence of the *Clostridium stercorarium xylA* gene encoding a bifunctional protein with β-D-xylosidase and α-L-arabinofuranosidase activities, and properties of the translated product. *Biosci. Biotechnol. Biochem.* **57,** 268–272
36. Utt, E. A., Eddy, C. K., Keshav, K. F., and Ingram, L. O. (1991) Sequencing

and expression of the *Butyrivibrio fibrisolvens xylB* gene encoding a novel bifunctional protein with β-D-xylosidase and α-L-arabinofuranosidase activities. *Appl. Environ. Microbiol.* **57,** 1227–1234
37. Pons, T., Naumoff, D. G., Martínez-Fleites, C., and Hernández, L. (2004) Three acidic residues are at the active site of a β-propeller architecture in glycoside hydrolase families 32, 43, 62, and 68. *Proteins* **54,** 424–432
38. Davies, G., and Henrissat, B. (1995) Structures and mechanisms of glycosyl hydrolases. *Structure* **3,** 853–859
39. Jordan, D. B., and Li, X. L. (2007) Variation in relative substrate specificity of bifunctional β-D-xylosidase/α-L-arabinofuranosidase by single-site mutations. Roles of substrate distortion and recognition. *Biochim. Biophys. Acta* **1774,** 1192–1198
40. Yoshida, S., Hespen, C. W., Beverly, R. L., Mackie, R. I., and Cann, I. K. (2010) Domain analysis of a modular α-L-arabinofuranosidase with a unique carbohydrate binding strategy from the fiber-degrading bacterium *Fibrobacter succinogenes* S85. *J. Bacteriol.* **192,** 5424–5436
41. Yamaguchi, A., Tada, T., Wada, K., Nakaniwa, T., Kitatani, T., Sogabe, Y., Takao, M., Sakai, T., and Nishimura, K. (2005) Structural basis for thermostability of endo-1,5-α-L-arabinanase from *Bacillus thermodenitrificans* TS-3. *J. Biochem.* **137,** 587–592
42. Brunzelle, J. S., Jordan, D. B., McCaslin, D. R., Olczak, A., and Wawrzak, Z. (2008) Structure of the two-subsite β-D-xylosidase from *Selenomonas ruminantium* in complex with 1,3-bis[tris(hydroxymethyl)methylamino]-propane. *Arch. Biochem. Biophys.* **474,** 157–166
43. Barker, I. J., Petersen, L., and Reilly, P. J. (2010) Mechanism of xylobiose hydrolysis by GH43 β-xylosidase. *J. Phys. Chem. B* **114,** 15389–15393
44. Burstein, T., Shulman, M., Jindou, S., Petkun, S., Frolow, F., Shoham, Y., Bayer, E. A., and Lamed, R. (2009) Physical association of the catalytic and helper modules of a family-9 glycoside hydrolase is essential for activity. *FEBS Lett.* **583,** 879–884
45. Richards, F. M. (1958) On the enzymic activity of subtilisin-modified ribonuclease. *Proc. Natl. Acad. Sci. U.S.A.* **44,** 162–166